SAND2018-10789R

Built on LDRD Laboratory Directed Research and Development

SAND

LDRD PROJECT NUMBER: 204724

LDRD PROJECT TITLE: Renewable hydrogen production via thermochemical/electrochemical coupling

PROJECT TEAM MEMBERS: Andrea Ambrosini (8823), Sean M. Babiniec (1514), James E. Miller (currently Arizona State University)

ABSTRACT:

A coupled electrochemical/thermochemical cycle was investigated to produce hydrogen from renewable resources. Like a conventional thermochemical cycle, this cycle leverages chemical energy stored in a thermochemical working material that is reduced thermally by solar energy. However, in this concept, the stored chemical energy only needs to be partially capable of splitting steam to produce hydrogen. To push the reaction to completion, a proton-conducting membrane is employed to separate hydrogen as it is produced, thus shifting the thermodynamics toward further hydrogen production. This novel coupled-cycle concept provides several benefits. First, the required oxidation enthalpy of the reversible thermochemical material is reduced, enabling the process to occur at lower temperatures. Second, removing the requirement for spontaneous steam-splitting widens the scope of materials compositions, allowing for less expensive/more abundant elements to be used. Lastly, thermodynamics calculations suggest that this concept can potentially reach higher efficiencies than photovoltaic-to-electrolysis hydrogen production methods. This Exploratory Express LDRD involved assessing the practical feasibility of the proposed coupled cycle. A test stand was designed and constructed and proton-conducting membranes were synthesized. An LDRD plus-up of $10k enabled the remediation of a membrane sealing issue and enabled testing with an improved membrane. However, the membrane proved too thick for efficient proton conduction, and there were insufficient funds to continue. While the full proof of concept was not achieved, the individual components of the experiment were validated and new capabilities that can be leveraged by a variety of programs were developed.

INTRODUCTION

Thermochemical cycles operate on the concept of converting thermal energy into chemical energy to drive subsequent chemical reactions. In brief, these cycles operate in two steps (Figure 1). In the first step, a “working” metal oxide material is heated above a temperature at which oxygen evolves from its crystal lattice, leaving behind oxygen vacancies. This leaves the material in a reduced state, where the thermal energy has been converted to chemical energy, represented by the material’s affinity to reincorporate oxygen into its structure. In a second, lower-temperature step, the material is exposed to steam, where the oxygen in steam has a higher affinity to bond with the reduced metal oxide than it does to remain bound with hydrogen atoms in hater, which oxidizes the metal oxide and yields H_2. The names “oxygen carrier” and “redox material” are attributed to the ability for the material to lose and gain oxygen as well as transport chemical energy in the reduced state or oxygen in the oxidized state.

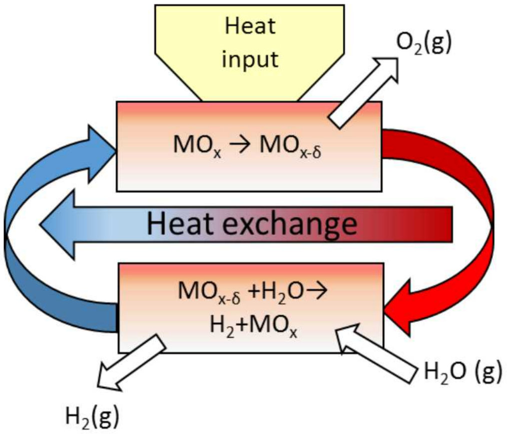

Figure 1: *Illustration of a two-step thermochemical cycle.*

Various metal oxide systems have been investigated as working materials for thermochemical cycles. These range from simple metal oxide pairs (ferrites, cobalt, Zn/ZnO), to blended oxides (cobalt ferrites), to mixed-ionic/electronic conducing (MIEC) oxides (ceria), to engineering perovskite MIECs[1,2,3,4]. One of the most successful steam-splitting redox materials is ceria due to its outstanding reaction kinetics and adequate thermodynamics to spontaneously split steam[3]. As these materials are reversible, the more affinity the material has for oxygen (increasing ability to split steam), the more difficult it is to remove the oxygen to reduce the material. This thermodynamic quantity is known as the reduction enthalpy. In the case of ceria, a reduction temperature of 1725 °C in air is required to achieve modest reduction of CeO_2 to $CeO_{1.95}$[5,6]. These extremely high temperatures and small reduction capacities result in limited choices for reactor construction materials, incompatibilities between the working material and reactor, limited choice of solar platforms, and reduced efficiencies.

In order to avoid the issues with reduction at such high temperatures, it is our goal to promote steam splitting *without* the requirement of spontaneous steam-splitting thermodynamics. This allows for a wide range of working materials options that exhibit lower reduction temperatures as well as enable the option to engineer materials to make them less expensive (by choosing earth-abundant cations) and to tune their performance (through material doping). However, in order to fully realize hydrogen production, the deficit in thermodynamic potential between the working material and steam splitting must be accounted for by another process. Our work focuses on coupling a proton-conducing membrane (PCM) to the thermochemical cycle in which the additional thermodynamic potential is electrically applied to the membrane, which operates as an electrochemical cell. This concept is coined “Electrically Enhanced Thermochemical Hydrogen Production”, or EETHP.

Thermodynamically, the two-step cycle can be written as:

$$\text{Reduction: } 1/\delta\, ABO_3 + \Delta H_{red} \leftrightarrow 1/\delta\, ABO_{(3-\delta)} + 1/2\, O_2 \quad (1)$$

$$\text{Oxidation: } 1/\delta\, ABO_{(3-\delta)} + H_2O \leftrightarrow 1/\delta\, ABO_3 + H_2 \quad (2)$$

Sandia National Laboratories is a multimission laboratory managed and operated by National Technology and Engineering Solutions of Sandia LLC, a wholly owned subsidiary of Honeywell International Inc. for the U.S. Department of Energy’s National Nuclear Security Administration under contract DE-NA0003525.

where δ is the oxygen non-stoichiometry in the material, otherwise known as the oxygen vacancy site concentration.

In either the direct thermochemical cycle or the EETHP cycle, Equation 1 remains the same, except that the magnitude of ΔH_{red} differs, as EETHP does not require reduction so thermodynamically deep as to be able to spontaneously split steam. In the unassisted thermochemical cycle, the material must be reduced deeply enough that the oxidation reaction occurs spontaneously, such that stoichiometric amounts of water and δ produce H_2. This is not the case in EETHP. Instead, small equilibrium concentrations of H_2 are produced, since the reduction enthalpy is not large enough to make the reaction spontaneous. However, the additional thermodynamic potential (ΔG) required to enable the reaction is provided by the electrochemical cell. Therefore, Equation 2 could be modified as such:

$$\text{Oxidation: } 1/\delta\, ABO_{(3-\delta)} + H_2O \ + \Delta G_{elect} \leftrightarrow 1/\delta\, ABO_3 + H_2 \quad (3)$$

where ΔG_{elect} is the Gibb's free energy associated with the electricity provided to the electrochemical cell. This concept can be visualized in Figure 2. If the oxidation of the working material in steam is not spontaneous, there will be a very small amount of hydrogen produced and then hydrogen production will stop once equilibrium is reached (Figure 2a). However, if the PCM is coupled, the hydrogen produced is continuously removed, preventing equilibrium concentrations from being reached, and hydrogen production is forced to continue (Figure 2b). This is commonly referred to as Le Chatelier's principle: reducing the concentration of products from a reaction shifts the reaction toward more products.

A full thermodynamic analysis was conducted to investigate the feasibility of the EEHTP concept[7]. This study assumed $SrMnO_{3-\delta}$ as the working material, primarily because it has a reduction enthalpy too low to split steam and the complete thermodynamic data for the material is published

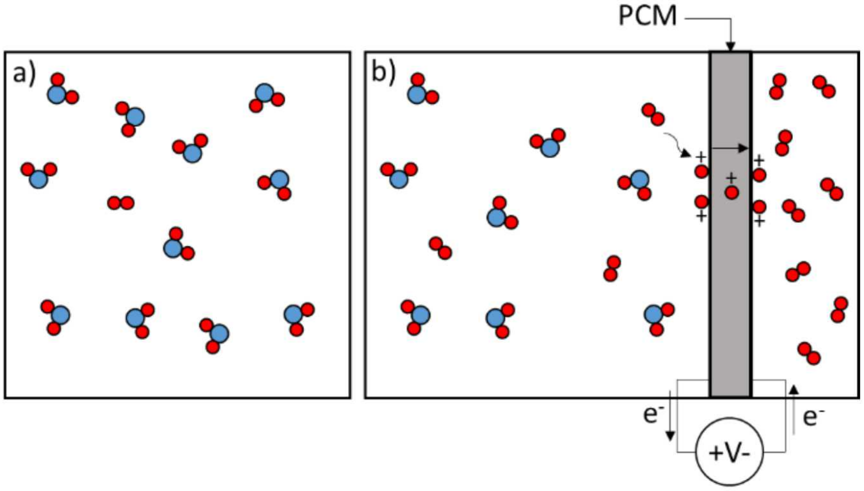

***Figure 2**: Illustration of non-spontaneous oxidation in steam (a) without coupled PCM, and (b) with coupled PCM.*

in the literature[8]. Not only did this study prove thermodynamic feasibility, but it also suggested high efficiencies of up to 25% for renewable hydrogen production.

Our primary technical objective for this project was to conduct a lab-scale proof of concept demonstration of the proposed idea with the following outcomes 1) demonstrate the validity of the chemical approach, and 2) provide validation of our thermodynamic calculations indicating the concept can be applied to split water with high efficiency.

DETAILED DESCRIPTION OF EXPERIMENT/METHOD

To investigate coupled oxidation of the working material, several facets of experimentation had to be addressed. These include test stand construction, materials synthesis and cell fabrication, electrochemical testing, and gas analysis.

Materials synthesis: The proton-conduction membrane (PCM) synthesized for the test cell was $BaCe_{0.1}Zr_{0.8}Y_{0.1}O_{3-\delta}$ (BCZY18), a known proton conducting electrolyte[9,10]. The material was synthesized using a Pechini solution method, wherein stoichiometric (metals basis) amounts metal nitrate/oxynitrate hydrate precursors were dissolved in H_2O with citric acid as a chelating agent. $Ni(NO_3)_2 \cdot 6H_2O$ was also added (corresponding to a 1 wt.% NiO concentration) to facilitate sintering, as a fully dense, gas-tight membrane is required for effective operation of the membrane. The solution was heated with stirring until most of the H_2O evaporated and a viscous gel formed. The gel was dried overnight at 100 °C, resulting in a dried foam. The nitrates were burned off by heating the foam, resulting in a fine powder of intimately-mixed metal oxide. The powder was calcined for several hours at 800 °C to remove any remaining organics/nitrates, and the resulting powder was sieved to obtain particles < 90 μm in size. The powders were mixed with 2-4 wt.% polyvinyl butyral binder and ground with an agate mortar and pestle. The resulting mixture was pressed into a 25 mm diameter pellet (approx. 1-2 mm thick) and sintered for 48 hours at 1375 °C. (This temperature is the upper limit of our in-house furnace.) When this temperature seemed insufficient, subsequent membranes were sintered an additional 24-48 hours at 1600 °C using a different furnace located at Sandia's Advanced Materials Lab.

$CaAl_{0.2}Mn_{0.8}O_{3-\delta}$ (CAM28) working material was also synthesized using a solution Pechini method. Stoichiometric amounts of nitrate salts were dissolved in water, then citric acid was added to the solution in a 1:1 molar cation:citric acid ratio. The solution was dried and combusted, and the resulting ash was pre-calcined at 850 °C for 2 hours in air. These powders were mixed with 1.5 wt.% polyvinyl butyral (PVB) and pressed in a ⌀ 13 mm die at 35 MPa. Pressed pellets were sintered at 1250 °C for 48 hours in air. The resulting product, which crystallizes in the orthorhombic perovskite structure (identified using X-ray powder diffraction), was then ground up into powder and sieved to the desired particle size for use in the electrochemical cell.

Test stand construction: The test stand was constructed using a ATS 3210 split-tube furnace mounted in a Unistrut cage. Custom alumina manifolds were machined by O'Keefe Ceramics to accommodate a 1" electrochemical cell and mate to ¾" alumina tubes (Figure 3). Gas delivery and electrical feedthroughs were fabricated using PTFE disks and were sealed via O-rings in the cold

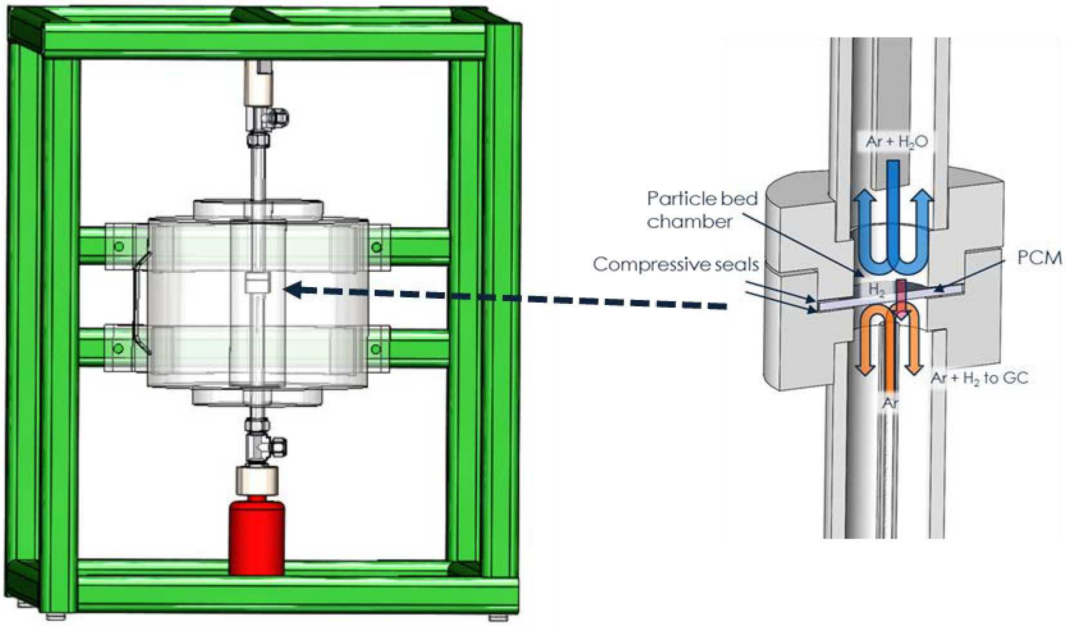

Figure 3: *Design of compressively-sealed test stand (left) and detail of manifold design (right).*

zone of the test stand. Hot zone seals within the alumina manifolds were accomplished using Flexitallic Thermiculite 886 compression seals. Argon was delivered to the top and bottom sides of the cell through Agilent mass-flow controllers (MFCs) capable of 0-500 ml/min gas flow. The top gas stream was also switchable to 2.9% H_2/ Ar balance with the option to humidify the gas stream through a bubbler chamber filled with DI water. A manifold was designed at the output to send either the top or bottom side to gas analysis or venting, whichever is required by the particular test being conducted.

<u>*Electrochemical cell fabrication:*</u> To construct the electrochemical cell, the membrane was placed in the manifold with compressive seals on either side. Silver mesh (99.999%) was used as an electrode and silver paste (ESL, Inc) was used to attach four-point electrical contacts fabricated from silver, such that there is both a current collect/supply wire and a voltage probe wire on each side of the cell. 1-2 grams of CAM28 powder were placed into the particle bed chamber on reactive (H_2/Ar or steam) side of the cell. The membrane cell was assembled into the test cell, which was then plumbed with the necessary gases and placed in a vertical tube furnace. (Figure 4)

<u>*Electrochemical measurements and gas analysis:*</u> Electrochemical experiments were driven by a Solartron 1287 potentio/galvanostat. Open-circuit voltage was measured during cell heating and during gas environment changes. The cell was polarized in a galvanostatic fashion, where a constant current was applied in the direction of promoting hydrogen transport while the voltage was monitored. Concurrently, the gas composition was monitored with an Agilent G2082A micro

gas chromatograph (μGC) utilizing a Molsieve column with Ar carrier gas to quantify evolution or consumption of gas species.

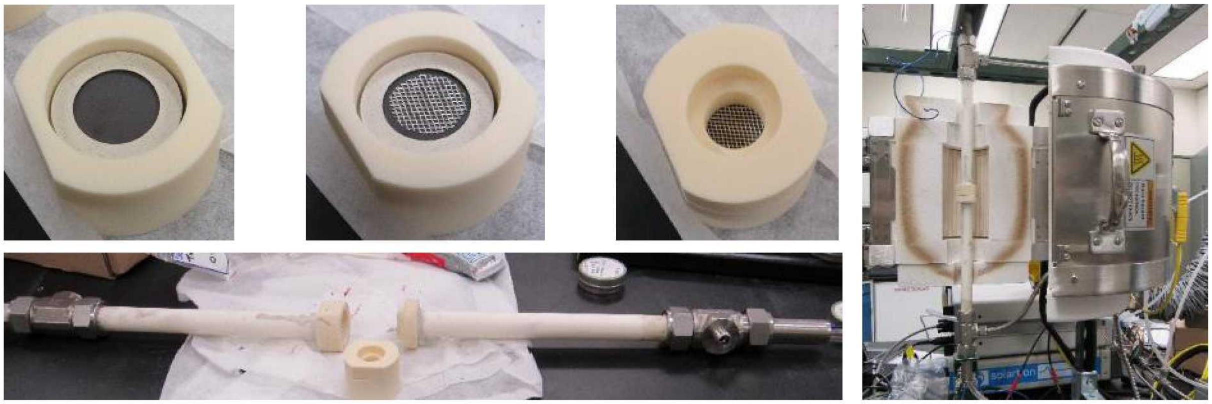

Figure 4: *Assembly of membrane cell (Top) and test cell (Bottom). Right: assembled test cell plumbed and in furnace.*

RESULTS:

The thermo-electrochemical test stand was designed and constructed as described and illustrated above. The test cell was successfully heated to 650 °C, and the connections, plumbing, gas flow, electrode connections, and gas analyses were verified to operate at temperature.

Producing a non-porous (> 90% theoretical density) flat PCM of BCZY18 was more challenging than anticipated. The first attempts, which involved pressing the calcined precursor powder into 25 mm disks and sintering at 1375 °C, resulted in warped porous discs that were unusable in the test cell. New membranes were synthesized, and an extra sieving step was added after the addition of binder. The powder was sieved to achieve particle sizes $\leq$ 90 μm in order to assure more homogeneous particle size and achieve less warpage and higher density. After sintering at 1375 °C, the membranes were less warped, but still porous. The membranes were sintered again at 1600 °C, resulting in slightly denser membranes, but were not completely gas impermeable. Dip-coating the sintered pellets in precursor nitrate solution followed by an additional 8-hour sinter at 1375 °C was attempted to fill the pores, but full density was still not achieved. In the interest of deadlines, however, experiments were conducted with the most promising-looking membranes.

The open circuit behavior of the cell was measured while flowing 2.9% H_2/Ar on the reactive side and an Ar sweep on the other. The agreement between the measured value versus the predicted behavior is shown in Figure **5**. In addition, an open circuit voltage (OCV) was observed when the feed gas was switched from 2.9% H_2/Ar to steam/Ar. A small presence of H_2 was detected in the presence of steam via gas chromatography, indicating that the reduced thermochemical working material (CAM28) was at least partially active.

The next step was to verify that the proton conducting membrane (PCM) of BCZY18 was effectively transporting hydrogen. This was initially performed by exposing the reactive side of

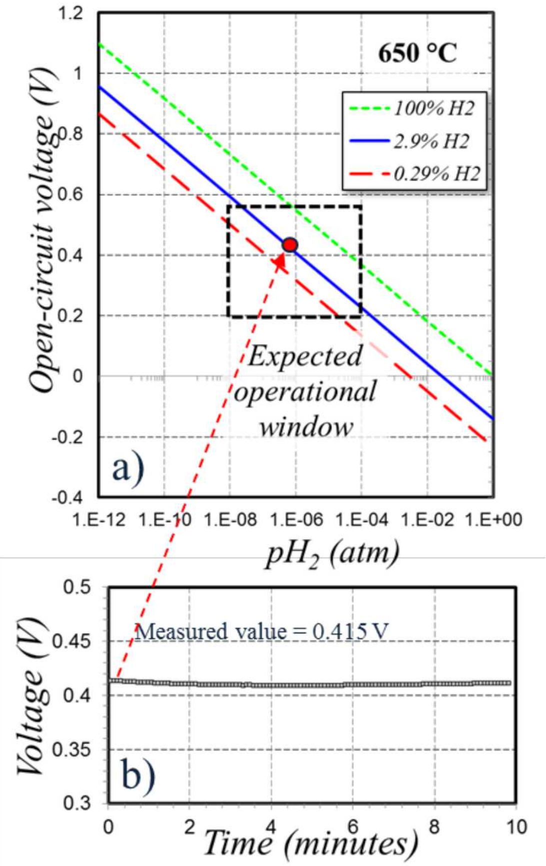

Figure 5: *(a) OCV as a function of pH2 on sweep side. (b) Measured open-circuit voltage.*

the cell to H_2/Ar and detecting the transported H_2 on the Ar sweep side of the cell. However, this planned experiment was thwarted by the presence of large O_2 and N_2 peaks on the μGC, indicating the presence of air, likely from a leak. Attempts to locate and ameliorate the leak were unsuccessful. No leak was observed on the active side of the cell. Therefore, an alternative experiment was designed and executed, which involved monitoring the concentration of H_2 on the H_2/Ar active side as a function of current. Theoretically, as the current to the membrane increases, so should the proton transport across the PCM. This should result in a decrease in H_2 concentration of the H_2/Ar gas on the active side of the electrochemical cell. Figure 6 shows the percentage of H_2 in the sweep gas, calculated from the decrease observed via μGC in the H_2 concentration in 2.9% H_2/Ar, versus current. While there is a slight increase in concentration, it does not reach the calculated Faradaic limit. However, the change in concentration does illustrate that some hydrogen transport is taking place.

In order to prove successful thermochemically-assisted hydrogen production, it must be shown that hydrogen is (1) produced from steam and (2) transported across the PCM. Due to the aforementioned leak on the sweep side of the cell, direct measurement of H_2 transport was not possible. Instead, the voltage at a given current was observed over a duration of several hours. The hypothesis behind this experiment was that if hydrogen production is thermochemically-assisted, the observed voltage should increase when the available thermochemical inventory is consumed, i.e., when the reduced working material is fully reoxidized by steam. The amount of the CAM28 working material was estimated to last for 3 hours of H_2 production assuming a Faradaic efficiency of 1.0; therefore, the experiment was set to run for 5 hours to ensure completion. Figure **7** shows the expected behavior versus the observed performance of the test cell. It is evident that the expected increase in voltage was not observed after five hours.

Leveraging pre-existing relationships, dense BCZY18 disks were provided to us by Colorado School of Mines (CSM), and a $10k plus up was granted to this exploratory LDRD to continue testing with the new membranes. The pellets are polished to a mirror-like finish, and no pores are observable, indicating very dense pellets. (Figure **8**) The pellets are 2.5 cm in diameter, with a

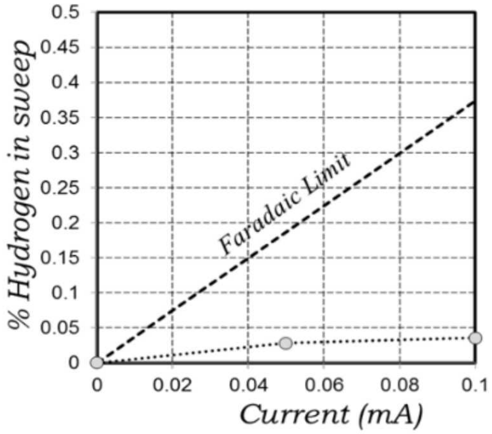

Figure 6: *Hydrogen transport performance: 2.9% H_2/bal. Ar vs. Ar, 650 °C.*

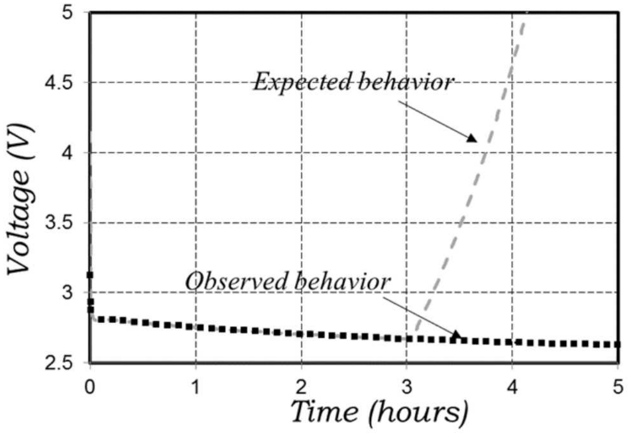

***Figure** 7: Expected vs. observed behavior of voltage over reaction time during assumed thermochemically-assisted H_2 production.*

thickness of approximately 2 mm, allowing them to act as a thick, monolithic membranes without the need of a support, unlike with thinner membranes. With improvements to the sealing methods, the original experiments were reinvestigated to observe the performance of the thick, dense membranes in more controlled environments. The improved membrane density and sealing are evidenced in Figure 9, where the hydrogen supplied to the top side does not leak across the membrane or membrane seals to the bottom side. A very small air leak was detected from the bottom side, but is negligible in scale.

Figure 8: *BCZY18 membrane pellets, (a) synthesized at Sandia and (b, c) from Colorado School of Mines. The image in (c) shows the reflection of the fluorescent light, an indication of the high density of the pellet.*

The open circuit voltage falls within the expected range at 650 °C (operational window in Figure 5 as compared to data in Figure 10, suggesting that electrochemical performance is as expected in open-circuit operation. As before, the cell was loaded with 2 g of reduced CAM28 powder. Hydrogen transport experiments were conducted at 10, 20, 30, and 40 mA (0.0079, 0.0158, 0.0237, and 0.0316 A/cm^2, respectively). The measured hydrogen production and subsequent transport are reported in Figure 11. Again, the produced hydrogen is far below the theoretical limit of hydrogen

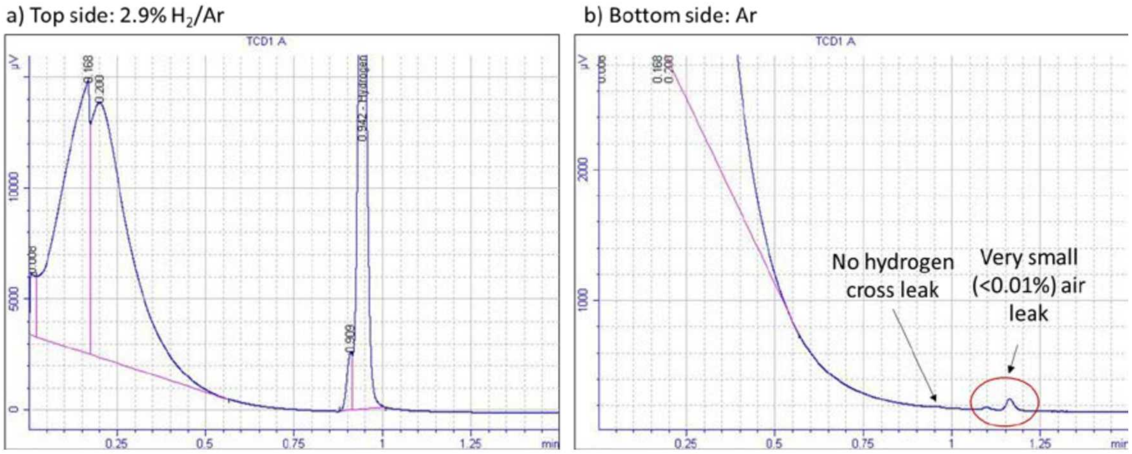
a) Top side: 2.9% H_2/Ar

b) Bottom side: Ar

Figure 9: *Gas chromatograph measurements at (a) hydrogen side (top side) and (b) sweep side (bottom side).*

transport across the membrane. This may indicate that steam splitting is a limiting factor, but the high voltages required to transport the hydrogen at each current were concerning. The left plot in Figure 12 shows the voltage response during the transport experiments (recall that OCV is +0.25 V). The voltage drops are very high. The 10, 20, and 30 mA currents show asymptotic behavior, suggesting that the membrane is stable. However, the 40 mA voltage shows a clear decrease as a function of time, indicating that degradation or crystallographic changes may be occurring in the membrane.

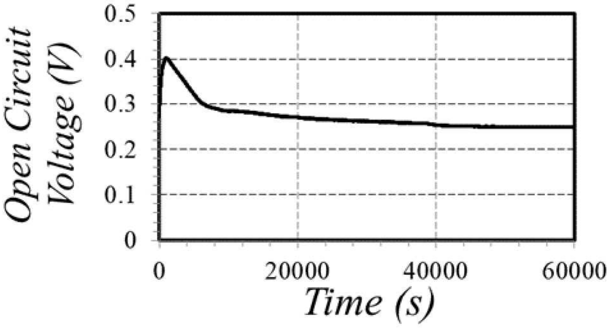

Figure 10: *Open circuit voltage in 2.9% H_2 vs Ar for CSM pellets*

The right plot in Figure 12 shows the observed voltage drops from OCV in each of the experiments. To ensure that the voltage drop was due to normal membrane resistance and not current collection or electrode issues, the expected voltage drop was calculated using conductivity data provided by Colorado School of Mines (Figure 13, left). By applying this data to our cell size, operating conditions, and operating temperature, the expected voltage drop can be calculated for a 2 mm thick membrane at 0.032 A/cm^2 current density. The voltage drop is calculated to be just below 5 V; the observed voltage drop was ~4 V, indicating a reasonable voltage loss due to ohmic resistance in the cell. Therefore, it is concluded that the thick, 2 mm cell is inadequate for hydrogen production purposes via thermochemically enhanced methods, as the measured voltage is higher than the voltage required to split steam. The applied high voltages are also damaging to the membrane and electronic transport dominates, as evidenced by the low transport efficiency. A thin

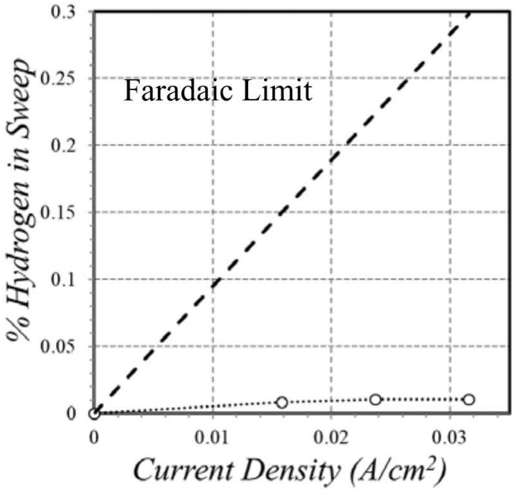

***Figure 11**: Hydrogen transport using CSM membrane. Symbols are measured data; black dashed line is the theoretical Faradaic limit.*

membrane supported cell, with a membrane thickness of ≤ 50 µm, would result in a voltage drop of 0.15 V, far lower than the electrolysis voltage. Such a design will be necessary going forward.

Despite less than optimal results, hydrogen production/transport experiments were still attempted in this cell configuration. The gas delivery to the top chamber was switched to humidified argon, the bottom was maintained at a sweep of argon, and the cell temperature remained constant at 650 °C. A 30 mA current (0.0237A/cm^2 current density) was applied to the cell, and the voltage drop was measured at 3.2 V during the experiment. During the experiment, the peak area % of the oxygen peak (from the small leak) clearly decreased during application of the current, and recovered when the current was turned off (Figure 14). The nitrogen peak exhibited no such change, implying that hydrogen was produced, transported across the membrane, and then reacted with the available air on the sweep side. However, the amount is too small to reliably quantify, and due to the high voltage drop observed, it is not possible to ascertain if the hydrogen was produced from electrolysis or the thermochemical reaction.

The membrane eventually degraded when water from the bubbler accumulated in the lines and migrated into the heated zone, rapidly expanding into a gas and cracking the membrane. Testing was halted at this point, due to time constraints and depleted plus-up funds.

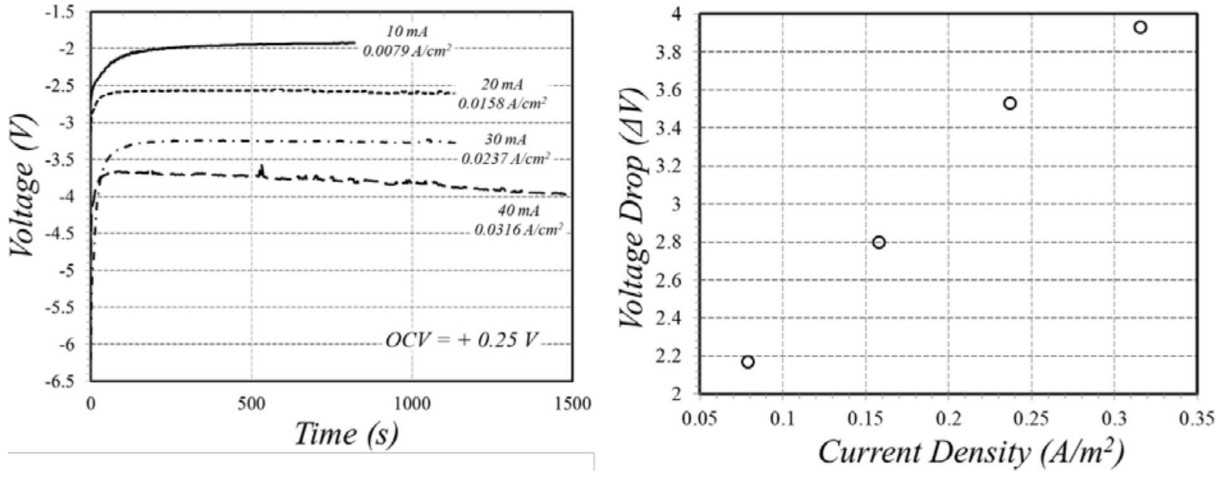

***Figure 12**: (Left) Voltage behavior over the duration of the hydrogen transport experiment. (Right) Voltage drop vs. OCV at each current density.*

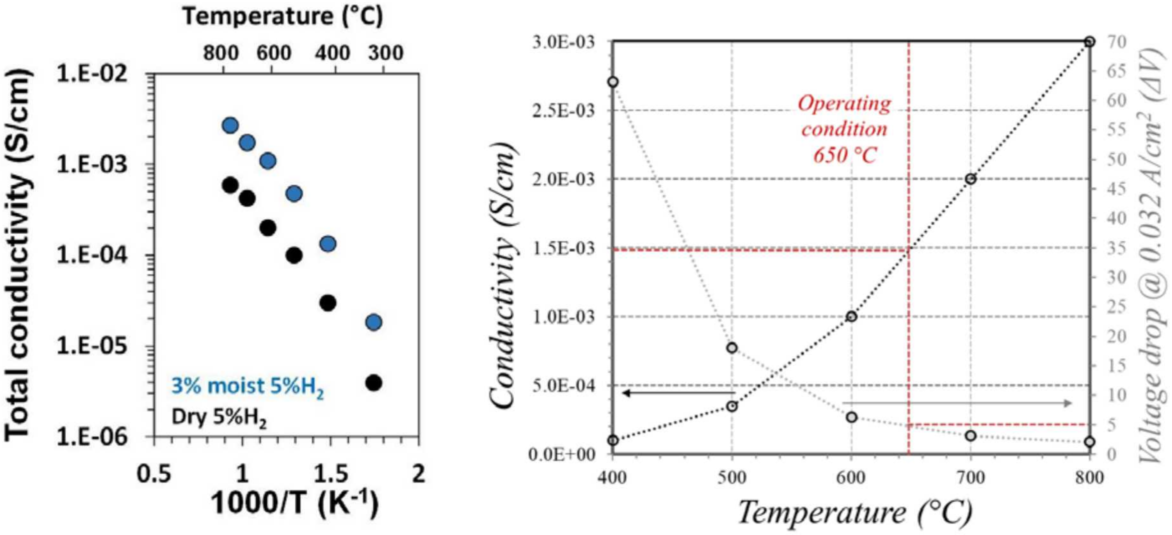

Figure 13: *BCZY18 conductivity (left) data measured by Colorado School of Mines, (right) data applied to the temperature and current density the hydrogen transport experiments.*

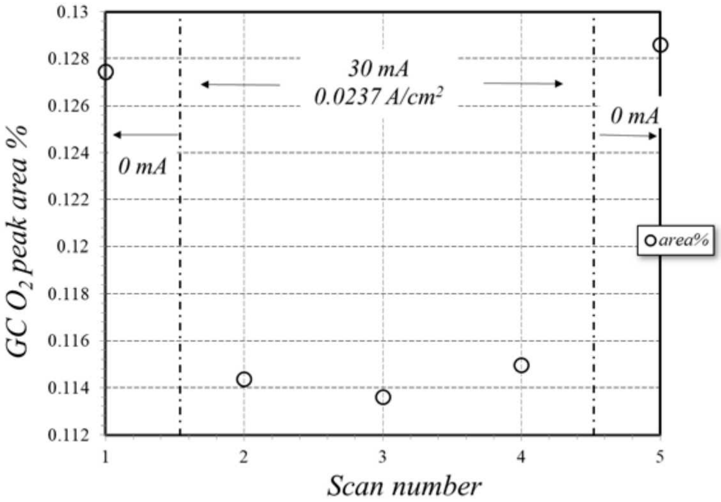

Figure 14: *Oxygen leak area percentage changes as current applied to cell, indicating produced/transported hydrogen reacting on the sweep side.*

DISCUSSION:

Working materials: BCZY18 and CAM28 were chosen as the PCM and thermochemical working materials, respectively, due to the team's familiarity with the materials. BCZY18 has a proven track record as a proton conductor [9,10]. CAM28 has been extensively studied and characterized as a redox-active material for thermochemical heat storage for concentrating solar power [11]. The thermodynamic properties of CAM28 are such that it theoretically should split water under the thermo- and electro-chemical conditions present in the test cell.

Challenges were encountered in synthesizing fully-dense, flat membranes of BCZY18 using the facilities at hand. Powder x-ray diffraction confirmed that the expected perovskite phase was obtained. Sieving the particles to reduce size distribution and pressing thicker membranes proved helpful in limiting the warpage, but were not sufficient to fully densify the membrane. One likely cause is the sintering temperature. In literature preparations, BCZY compositions were coated onto supports and sintered at 1600 °C. The presence of a support likely inhibits warpage and results in better sintering. In our case, the material was made as a stand-alone membrane and originally sintered to 1375 °C, due to temperature limits in the available furnace. It was hoped that the intimate mixing and small particle size of the precursor powders obtained by the Pechini solution prep (vs. solid state methods) would compensate for the lower sintering temperature, which was not the case. Post-sintering at 1600 °C did not solve the issue; it's possible that the second sintering step was ineffective due the loss of binder and NiO sintering aid during the first step. In other words, the microstructure that formed at 1375 °C could not be overcome by additional heating. Additional attempts to optimize the membrane would have resulted in unacceptable project delays, and it was decided to move forward with most promising membranes amongst the synthesized cohort.

Electrochemical cell performance: The open circuit behavior of the cell was calculated as a function of partial pressure of H_2 on the sweep side of the call at 650 °C (Figure 5a) for several concentrations of H_2 on the active side. The area of interest for this set of experiments is found in the boxed area. The observed OCV under the experimental conditions of 2.9% H_2/Ar fits well with the calculated value (**F**igure 5b), indicating that the membrane is electrochemically active, despite the presence of porosity. An OCV was also observed when the feed gas was switched to steam/Ar. In addition, a small amount of H_2 was detected via μGC on the active side, implying that the CAM28 working material is also active.

The proton conducting properties of the BCZY18 membrane were investigated electrochemically, by measuring the flux of protons through the PCM as a function of current. Since membrane/seal leakage prevented the direct measurement of H_2 evolution on the sweep side, the H_2 concentration on the active side of the cell was measured, under the assumption that transport of protons across the PCM to the sweep side would result in a decrease of H_2 on the active side. Figure 6 shows the results. A slight increase in current was measured, indicating some proton transport, but it does not approach the calculated Faradaic efficiency of the cell membrane. The observed low Faradaic efficiency can be attributed to several possible causes related to cell assembly. These include a poor membrane seal, either due to slight warpage or faulty O-ring. This may also be the source of the leak detected on the sweep side of the test cell. The porosity of the membrane may also play a role in the poor performance. Finally, there may be electronic leakage in the membrane as a result of additional charge carriers (electrons, holes, and/or oxides) which may form as a function of gas environment and voltage. While normal operating conditions should not favor additional carrier formation, the presence of air due to a leak may result in their creation.

A second membrane, provided by the Colorado School of Mines, was tested in our experimental setup. This cell was extremely dense, but also 2 mm thick. Hydrogen transport was observed with very low Faradaic efficiency. The thickness of the pellet required very high voltages to drive current across the membrane, which have been shown to result in electronic defect formation through a change in the valence state of cerium[9]. It is hypothesized that this is the reason for poor hydrogen transport.

Hydrogen production: The ultimate proof of concept of the theorized coupled thermochemical/electrochemical production of hydrogen via EETHP is to demonstrate that hydrogen is (1) produced from steam and (2) transported across the PCM. As described in the Results section, the existence of a leak on the sweep side of the cell prevented direct monitoring of hydrogen production via steam-splitting and subsequent transport across a proton conducting membrane. The alternate experiment to measure steam splitting activity via observing voltage over time (Figure **7**), with the expectation that the voltage would jump after the CAM28 fully reacted, also did not yield expected results. There can be several reasons for this: (1) Low faradaic efficiency resulted in decreased proton transport, and the thermochemical material was not fully oxidized by end of experiment. I.e., the water splitting reaction was not driven to completion due to lackluster proton transport through the PCM. (2) The thermochemical working material did not adequately reduce at 650 °C under 2.9% H_2/Ar. Although thermodynamic calculations can accurately predict the extent of reduction of CAM28 at a given temperature and atmosphere, unintended exposure to air, e.g. from a leak, could cause unintended oxidation. (3) Kinetic limitations hindered thermochemical assistance, thus reoxidation of the working material by steam proceeded too slowly to be effective.

In follow-on experiments, indirect observation of hydrogen production was successful using the membrane provided by Mines. A clear trend in the oxygen peak was observed when a current was applied to the membrane, with no corresponding change in the nitrogen peak, suggesting that produced H_2 was transported through the membrane and reacted with oxygen on the sweep side, thus lowering the concentration. The high voltage associated with the hydrogen transport, however, makes it difficult to ascertain if the steam was split via electrolysis or thermochemical means, since the voltage applied to the membrane to effect transport exceeded that required for direct electrolysis.

CONCLUSION:

The milestone of this EE LDRD was to achieve the lab-scale demonstration of the EETHP concept that couples thermal/electrochemical hydrogen production to provide a renewable thermal route to hydrogen from water at system thermal efficiency of > 20% (including thermal equivalent of electrical demand) and a peak system temperature of < 1200 ºC. While the project fell somewhat short of this goal in the time allotted, several important results were realized. A novel test stand to prove the concept was conceptualized and constructed. The test cell was successfully heated to 650 °C without incident. Initial membrane warpage and insufficient sealing were overcome utilizing the $10k plus-up, allowing additional tests to proceed from which proton transport across a dense BCZY18 membrane was demonstrated, as was the water splitting activity of the CAM28 working material. In short, the individual components of the experiment were validated, but assembly issues and cell configuration issues hindered the success. We predict that a supported thin-film PCM is required for future testing, so that transport can occur at voltages lower than required for electrolysis, thus demonstrating the production of hydrogen solely by thermochemical water splitting. The thinner membrane will also allow for better proton transfer kinetics, resulting in faster in-situ hydrogen separation, preventing reaction equilibrium from being reached on the reaction side, and the lower required voltages will prevent potential damage to the membrane caused by such harsh operating conditions.

ANTICIPATED OUTCOMES AND IMPACTS

Next steps: Immediate steps that we would take going forward in order to meet our Milestone include the following:

- Use lessons-learned to fabricate improved membranes, with minimum porosity and warpage
    - Sinter directly to 1600 °C without intermediate 1375 °C step
    - Determine best precursor particle size and distribution to prevent warpage and maximize density
    - Decrease membrane thickness to < 100 μm, likely supported on a porous substrate
- Once membrane issues are resolved, repeat intended experimental set but this time obtain direct (versus implied) results by detecting and quantifying H_2 in Ar sweep gas. Verify:
    - Thermochemical activity of CAM28 working material
    - Proton transport through BCZY18 PCM
    - Thermochemically-assisted electrolysis is more efficient than electrolysis alone
- Analyze steam/H_2O concentrations in reaction cell for full characterization of gas streams
    - Current μGC configuration (Molsieve column) does not detect H_2O
    - Mass spectrometry could be utilized to fully characterize gas compositions

Future steps: After demonstrating proof of concept, we would propose these activities as part of any future funded projects.

- Fully characterize system by varying applied current, reduction extent of working material, reaction temperature
    - Quantify transport efficiency and kinetic limitations of PCM
    - Extract thermodynamic information: with denser membranes, OCV with and without thermochemical material could provide analysis of the change in thermodynamic state due to the presence of thermochemical material
- Materials development

  - Identify promising redox-active materials compositions from the broader the field enabled by lower reaction temperatures for thermochemical steam splitting
  - Leverage materials development efforts from SunShot-funded CSP thermochemical energy storage (PROMOTES), e.g., CAM28 and FCTO-supported solar thermochemical water splitting (STCH) programs
  - Investigate new materials compositions for proton conducting membranes

- Utilize the capabilities at the National Solar Thermal Test Facility (solar simulator, solar furnace) at Sandia to couple reactor to a concentrating solar power source to determine feasibility of developing a fully renewable process

Resulting publications/patents:

- Provisional patent: Patent No. 62/461,141 filed on 2 February, 2017
  - Full patent filed: Patent No. 15/899,295 file on 19 February, 2018
- Publications
  - S.M. Babiniec, A. Ambrosini, J.E. Miller, "Thermodynamic assessment of an electrically-enhanced thermochemical hydrogen production (EETHP) concept for renewable hydrogen generation", *Int. J. Hydrogen Energy* 42, 14380-14389, 2017.
  - Follow-on paper planned after more data is accumulated

Impact:

- The test stand is a new capability can be leveraged for testing a variety of application relevant to Sandia programs, such as solid oxide fuel cell/electrolyzer materials, thermochemical H_2 and fuels production, thermodynamic measurements of redox active materials
- Mission relevance: Directly addresses SNL's SSEF mission space and DOE and EERE mission areas, e.g. DOE's Fuel Cell Technology Office (FCTO) and HydroGEN Advanced Water Splitting Materials (HydroGEN AWeSoMe), for which Sandia is a core laboratory
- Successful demonstration of this process can enable increased efficiency of H_2 production utilizing renewable resources (CSP, PV, H_2O), which will enhance and secure America's energy future
- Increased visibility of Sandia R&D via publications and presentations at national conferences

Upcoming funding opportunities and partners:

Potential partners going forward include both internal Sandia departments including 8823 (NSTTF), 8367 (Hydrogen and Materials Science), and 1815 (AML), as well as external collaborators such as Colorado School of Mines (thermochemical energy storage, PCM development), Arizona State University (technoeconomic and systems analyses), and Georgia Institute of Technology (Academic Alliance, solar fuels and technologies).

Sandia is a core laboratory for DOE's HydroGEN Advanced Water Splitting Materials effort. The team will endeavor to find support within this energy materials network (EMN) both directly (i.e., internally) and as a resource to external partners. The team also intends to apply for an LDRD to perform necessary follow-on R&D, such as materials discovery and optimization, both computationally and conventionally, for both PCMs and active metal oxides, kinetic and thermodynamic characterization, and integration with renewable power sources. Several proposals based on the EETHP concept and preliminary results were submitted to FOAs from FCTO, Solar Energy Technologies Office (SETO), and ARPA-E.

---

[1] Roeb M, Neises M, Monnerie N, Call F, Simon H, Sattler C, et al. Materials-related aspects of thermochemical water and carbon dioxide splitting: a review. Materials 2012;5:2015-54. http://dx.doi.org/10.3390/ma5112015.

[2] Agrafiotis C, Roeb M, Sattler C. A review on solar thermal syngas production via redox pair-based water/carbon dioxide splitting thermochemical cycles. Renew Sustain Energy Rev 2015;42:254-85. http://dx.doi.org/10.1016/j.rser.2014.09.039.

[3] Miller JE, McDaniel AH, Allendorf MD. Considerations in the design of materials for solar-driven fuel production using metal-oxide thermochemical cycles. Adv Energy Mater 2014;4:1300469. http://dx.doi.org/10.1002/aenm.201300469.

[4] Scheffe JR, Steinfeld A. Oxygen exchange materials for solar thermochemical splitting of H2O and CO2: a review. Mater Today 2014;17:341e8. http://dx.doi.org/10.1016/j.mattod.2014.04.025.

[5] Zinkevich M, Djurovic D, Aldinger F. Thermodynamic modelling of the cerium-oxygen system. Solid State Ionics 2006;177:989-1001. http://dx.doi.org/10.1016/j.ssi.2006.02.044.

[6] Palumbo R, Larson C, Guertin J, Schoer J, Meyer M, Diver RB, et al. Solar thermal decoupled water electrolysis process I: proof of concept. Chem Eng Sci 2012;84:372-80. http://dx.doi.org/10.1016/j.ces.2012.08.023.

[7] Babiniec SM, Ambrosini A, Miller, JE. Thermodynamic assessment of an electrically-enhanced thermochemical hydrogen production (EETHP) concept for renewable hydrogen generation. Int. J. Hydrogen Energy 2017;42;14380-14389.

[8] Rørmark L, Mørch AB, Wiik K, Stølen S, Grande T. Enthalpies of oxidation of $CaMnO_{3-\delta}$, $Ca_2MnO_{4-\delta}$, and $SrMnO_{3-\delta}$ - deduced redox properties. Chem Mater 2001;13:4005-13.

[9] Babiniec SM, Ricote S, Sullivan NP. Characterization of ionic transport thought $BaCe_{0.2}Zr_{0.7}Y_{0.1}O_{3-\delta}$ membranes in galvanic and electrolytic operation. Int. J. Hydrogen Energy 2015; 30; 9278-9286.

[10] Dippon M, Babiniec SM, Ding H, Ricote S, Sullivan NP. Exploring electronic conduction through $BaCe_xZr_{0.9-x}Y_{0.1}O_{3-\delta}$ proton-conducting ceramics. Solid State Ionics 2016; 286; 117-121.

[11] Babiniec SM, Coker EN, Miller JE, Ambrosini A. Doped calcium manganites for advanced high-temperature thermochemical energy storage. Int. J. Energy Research 2016; 40; 280-284.